

Grain-size-dependent paleointensity results from very recent mid-oceanic ridge basalts

J. Carlut¹ and D. V. Kent²

Lamont-Doherty Earth Observatory, Paleomagnetic Laboratory, Palisades, New York, USA

Received 2 February 2001; accepted 7 October 2001; published 19 March 2002.

[1] We report paleointensity analyses on a suite of four samples from two axial zero-age mid-oceanic ridge basalt flows from the East Pacific Rise. Paleointensity experiments have been performed on several profiles, each consisting of a batch of small (millimeter scale) subsamples going from the rapidly cooled glassy margin to the interior. The Coe version of the Thellier double-heating procedure was used with back checks performed after every other heating step. Most of the samples show very good behavior, i.e., constant ratio between the lost and acquired magnetization through a large temperature range (quality factor usually above 10) and positive checks, which lead to unambiguous paleointensity determinations. Paleointensities obtained on glasses reported here and in a previously published study are very consistent and reproducible and in agreement with expected in situ values of Earth's magnetic field intensity. However, results found within the crystalline part of the samples show values that are considerably (up to 50%) higher than expected. These variations seem to be correlated with the cooling history of the samples and appear to be universal since all samples exhibit the same intriguing pattern. An extensive study of magnetic properties allows us to link this incongruent behavior to (1) the presence of multidomain effects and (2) the cooling rate difference between laboratory experiments and in situ cooling. *INDEX*

TERMS: 1512 Geomagnetism and Paleomagnetism: Environmental magnetism; 1540 Geomagnetism and Paleomagnetism: Rock and mineral magnetism; 3035 Marine Geology and Geophysics: Midocean ridge processes; *KEYWORDS:* Thellier, Multidomain, Exsolution, MORB, Titanomagnetite, Cooling rate

1. Introduction

[2] Detailed sea surface magnetic surveys have yielded the identification of consistent magnetic variations within chrons. It has been suggested that these “tiny wiggles” of magnetic profiles are directly associated with paleointensity variations [Cande and Kent, 1992; Gee *et al.*, 1996; Pouliquen *et al.*, 2001]. This requires that the magnetization of the upper layer of the oceanic crust is a high-fidelity recorder of the geomagnetic field. Several studies focusing on the paleointensity record in glasses were undertaken recently, and high-quality paleointensity results were obtained [Pick and Tauxe, 1993; Mejia *et al.*, 1996; Gee *et al.*, 2000; Carlut and Kent, 2000]. These results are consistent with rock magnetic observations that basaltic glass is a very good material to recover the absolute paleointensity value of the field [Pick and Tauxe, 1993; Zhou *et al.*, 1999]. However, magnetic anomalies are caused by basalts rather than glasses, and little is known about the paleointensity record in mid-oceanic ridge basalts (MORBs).

[3] Subaerial lavas are considered as a reliable recorder of the past intensity of the geomagnetic field, and our knowledge of the past variations of the field intensity is mainly achieved using this material. The rapidly cooled submarine flows which are supposed to have a more uniform magnetic grain size distribution are thus expected to also give accurate and well-constrained results. However, some authors have reported unusu-

ally high paleointensity values obtained on nonglassy MORB samples [Prévot *et al.*, 1983], while others found very low values [Grommé *et al.*, 1979; Dunlop and Hale, 1976]. The interpretation of such results was hampered by the absence of age control and the possible alteration undergone by the samples. One study on a flow that erupted in the Juan de Fuca area in 1993 (the so-called New Flow) showed Thellier paleointensity results consistent with the expected value [Kent and Gee, 1996]. Unfortunately, the area was later recognized as anomalous with very large local magnetic anomalies [Tivey *et al.*, 1998; Carlut and Kent, 2000]. Thus it is still unclear whether the crystalline part of MORB could yield accurate paleointensity values. Experiments made on very recent submarine flows constitute a critical test of the suitability of MORBs for paleointensity investigation. In this study we document detailed paleointensity results from the outer glassy margin [Carlut and Kent, 2000] to the interior on zero-age basalt samples.

2. Background and Samples

[4] We performed paleointensity analyses on one pillow from the “New Flow” erupted on the Juan de Fuca (JDF) area in 1993 (see Fox *et al.* [1995] for details about the eruption) and three lobate flows from the southern East Pacific Rise (SEPR). The magnetic properties of another pillow sample from the JDF New Flow were previously studied by Johnson and Tivey [1995] and Kent and Gee [1996]. The latter study raised several questions about the possible presence of a systematic multicomponent magnetizations and the reliability of paleointensity determinations on nonglassy samples. The New Flow sample used in this study, designated as R2-93 and recovered at ~46°31.68'N, 129°34.69'W, was made available to us by P. Johnson (University

¹Now at Laboratoire de Géologie ENS, Paris, France.

²Also at Department of Geological Sciences, Rutgers University, Piscataway, New Jersey, USA.

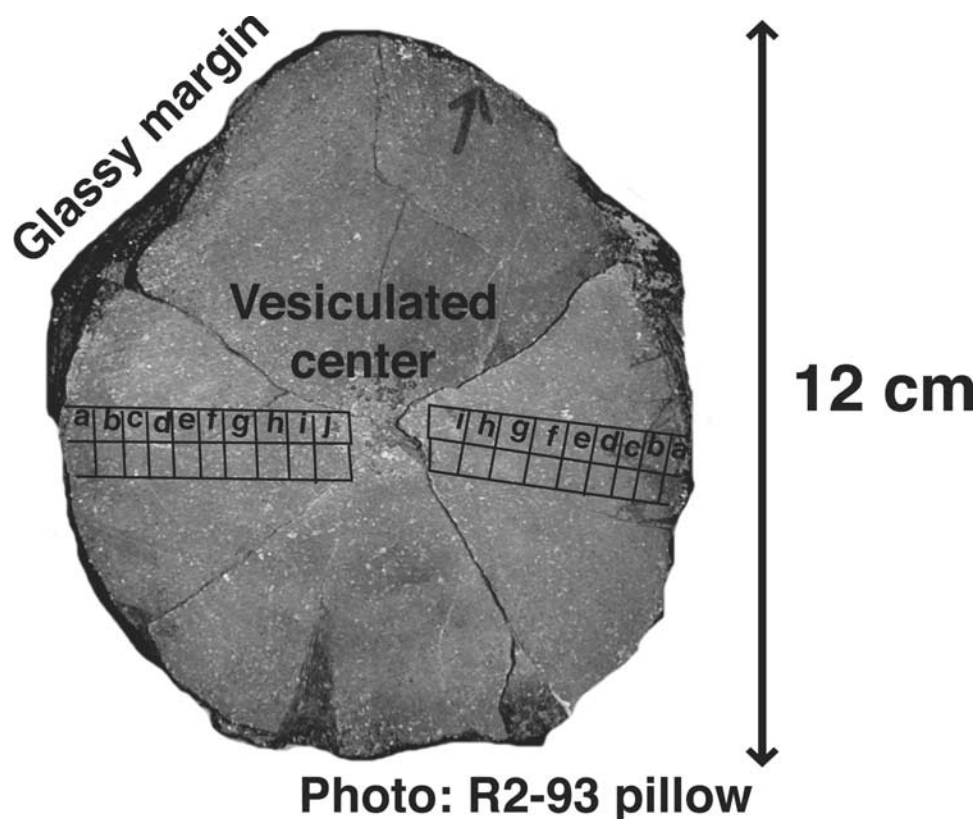


Figure 1. Photograph showing pillow sample R2-93. The subspecimens location is indicated.

of Washington). Paleointensity results on glassy chips extracted from this ~ 11 cm diameter pillow have been reported by *Carlut and Kent* [2000]. In addition, basalt samples from the Animal Farm flow (referred as AnF in the following) on the SEPR were also studied (see *Auzende et al.* [1994, 1996] for a description of the flow). They were collected between $18^{\circ}35'S$ and $18^{\circ}44'S$ during a dive of the Alvin in January 1999; three samples from three different locations were made available to us (M. Cormier and J. Sinton, personal communication). Each of these samples is of a lobate flow that exhibits two cooling margins, a glassy outermost part and an innermost vesiculated zone next to a cavity where water was probably circulating. The size of the samples (distance between outermost glassy rim and second cooling margin) are ~ 3 cm (sample 3349-2), ~ 5.5 cm (3346-15), and ~ 11 cm (sample 3344-6). Paleointensity results on the glassy part of samples 3349-2 and 3344-6 were reported by *Carlut and Kent* [2000].

[5] All fragments showed an outermost glassy rind of from 2 to 10 mm thick sometimes covered by a light brown coating on the outermost glassy surface (R2-93) surrounding a dark gray basalt which seems fresh on a cut surface. In the case of R2-93 a small vesiculated area marks the center of the pillow bud. Each sample was sliced perpendicularly to the outer margin. Columnar subsamples about 10 mm in cross section were cut radially from the outermost glassy part to the center in case of R2-93 or the other margin in the case of AnF fragments. Each of the columnar subsamples were divided into specimens at 5 (close to the glassy margin) and 10 mm depth intervals for measurements (see Figure 1). Small glass chips weighing about 30–100 mg were also extracted for measurements. To facilitate handling during magnetic measurements, the glassy subsamples were glued to microscope slides using the Kasil slide technique (as described by *Carlut and Kent* [2000]). The small basalt specimens were mounted on slides or sometimes encapsulated in pellets made

from ordinary table salt (the higher magnetization of the basalt allows salt encapsulation).

3. Determination of Absolute Paleointensity

[6] Paleointensity experiments were performed on a total of 51 subsamples, 6 of them being glassy (8 subsamples from 3349-2, 11 from 3344-6, 11 from 3346-15, and 21 from R2-93). The modified Thellier-Thellier double-heating method [*Thellier and Thellier*, 1959; *Coe*, 1967] was used with heating and cooling in air. Partial thermoremanent magnetization (PTRM) checks were performed systematically every temperature step. The laboratory field was set either to 33 or 40 μT , depending on the experiment. Measurements were made in a shielded room using a 2G cryogenic magnetometer.

[7] The success rate of the Thellier experiments was high in that 46 out of the 51 samples exhibit good Thellier paleointensity behavior, i.e., constant natural remanent magnetization (NRM)/PTRM ratio and positive PTRM checks (within 5% of the first PTRM) over a wide temperature range. Such a high rate would be atypical for subaerial basalts where a 15–30% success rate is more common [e.g., *Valet et al.*, 1996]. However, the MORB glass success rate is comparable to paleointensity results obtained from archeological artifacts which can be on the order of 80% or more [e.g., *Chauvin et al.*, 2000] and attests to the extreme freshness of the samples. Representative paleointensity experimental results in the form of Arai TRM/NRM diagrams [*Nagata et al.*, 1963] with their associated directional demagnetization diagrams (for ATV2) are shown in Figure 2. In almost all samples the primary directional component was successfully isolated after $100^{\circ}C$. The paleofield value was derived from the slope of the Arai diagram. Results for the 46 samples are summarized together with the fraction, gap, and quality factors [see *Coe et al.*, 1978; *Prévoit et al.*, 1985] in Table 1,

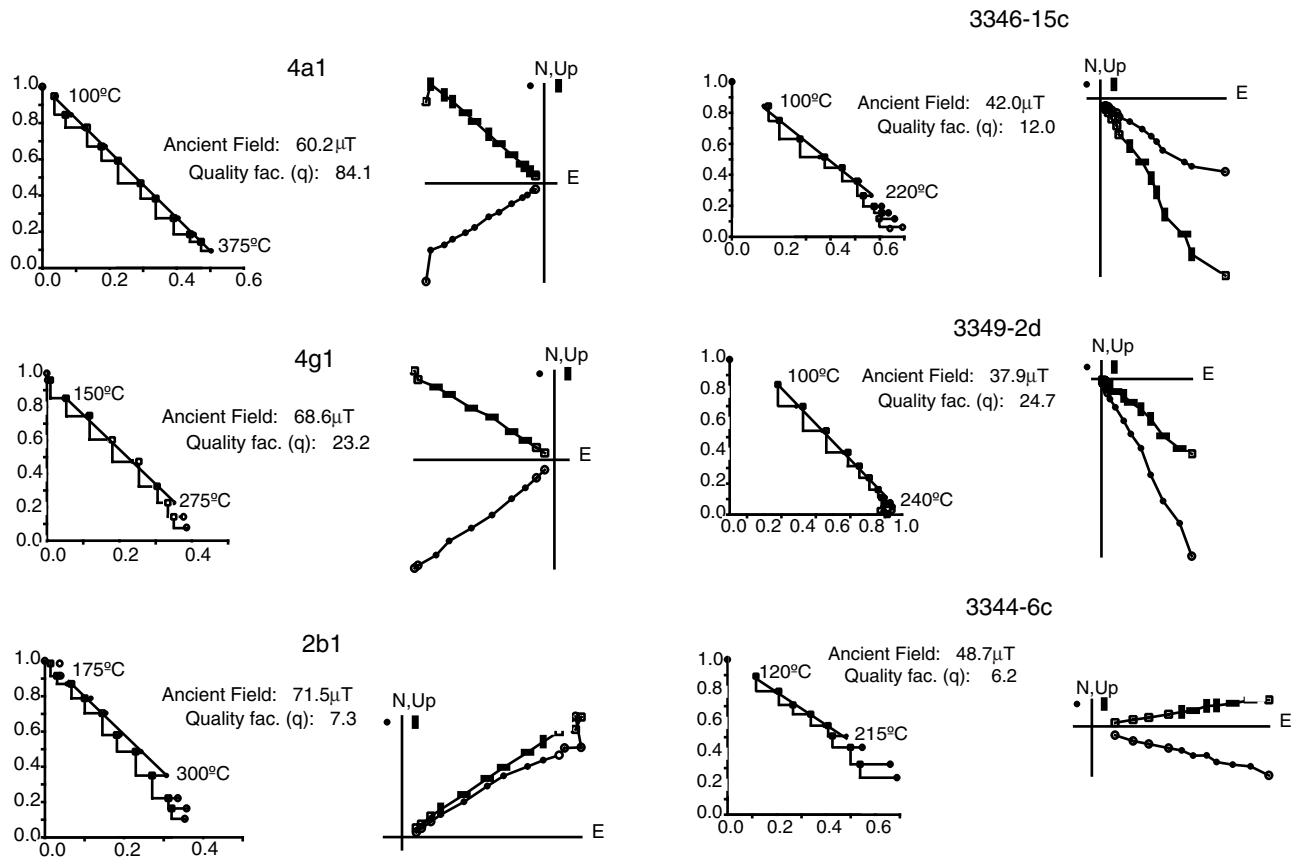


Figure 2. Natural remanent magnetization (NRM) versus thermoremanent magnetization (TRM) (Arai) diagrams for typical samples. Included for each sample are Zijderveld diagrams, squares corresponding to projections onto the horizontal plane, while circles are projections onto the vertical plane. Temperature steps are every 25°C.

which also includes a summary of the results previously obtained by *Carlut and Kent* [2000] on 17 glassy samples from R2-93, 3349-2, and 3344-6. The quality factor is often above 10, which attests to the high quality of this data set.

[8] When the results are plotted with respect to subsample distance from the glassy margin (Figure 3), it is apparent that the recovered paleointensity is not constant throughout the samples. All samples show the same sharp increase from the outer margin toward the interior (from 20 to 45% for the AnF samples and ~30% for R2-93) until a maximum is reached after 1 or 2 cm from the glassy margin, followed by a slower decrease in values. As apparent with the AnF samples, the magnitude of the maximum seems dependent on the size of the samples; the larger one (3346-15) shows values reaching 49 μT, the intermediate being 42 μT, while the maximum reached by the smaller one is only 38 μT. After 4 cm, 3346-15 and 3344-6 seem to give more stable and concordant values. A small decrease from the glasses to the first inner subsample (on the order of 10% for all AnF samples and 20% for R2-93) is also apparent.

[9] The pattern of elevated paleointensities below the chilled margin seems to be reproducible as four samples from two flows from different locations give identical trends. To understand this behavior the magnetic properties of the samples have been scrutinized.

4. Rock Magnetic Properties

4.1. Natural Remanent Magnetization

[10] Detailed profiles of NRM intensity with distance from the outer glassy margin were measured on a collection of

samples in addition to the one used for Thellier experiments. A thick glassy crust preserved over part of R2-93 sample allows a detailed “microstratigraphic” sampling from the outermost chips to the almost crystalline part. AnF samples may originally have had a thick glassy crust which was lost in recovery, thus no detailed sampling could be performed. Results are reported in the top and bottom of Figure 4 (for R2-93 and AnF, respectively). NRM intensity spans up to 4 orders of magnitude in each sample. It is apparent from these data that the glasses undergo very strong variations on a millimeter scale, the remanence increasing sharply in the first centimeter, whereas the innermost part of the samples depict much smoother variations. Similar phenomenon has already been reported in several studies [*Marshall and Cox*, 1971; *Kent and Gee*, 1996; *Gee and Kent*, 1999]. The very rapid cooling of the first few millimeters, which probably solidify in less than a few seconds [*Griffiths and Fink*, 1992], does not allow the crystallization of an important amount of magnetic minerals, as reflected by the low NRM values. The sharp NRM increase indicates a rapid formation of those minerals with only slightly lower solidification rates. After the first centimeter or so, the slower cooling leads to an apparent increase of the grain size which tends to decrease the magnetization, whereas the increasing proportion of crystallized magnetic minerals tends to increase magnetization; together, these phenomena can account for an overall smooth cooling-rate-dependent variation in magnetization [*Marshall and Cox*, 1971; *Kent and Gee*, 1996]. The variations throughout the samples strongly emphasize the difficulty to define a single NRM value characterizing each submarine flow. The magnetic susceptibility

Table 1. Results of Paleointensity Experiments

Sample	Success Rate ^a	Subsample ^b	Distance From Glassy Margin, cm	NRM, 10 ⁻³ A. m ² /kg	Number of Heating Steps Used	Temperature Range, deg. C	Fraction Factor	Gap Factor	Quality Factor	F _a , μT	Standard Error, μT	F _{tot} , μT	Standard Error, μT
R2-93	12/15	<i>Mean</i>										73.6	1.9
	17/21	4a1	0.25	1.369	11	100-375	0.85	0.89	84.1	60.2	0.5		
		4b1	0.55	5.498	10	150-375	0.69	0.88	19.5	71.5	2.3		
		4c1	0.9	14.49	5	225-300	0.31	0.66	2.6	79.1	2.8		
		4d1	1.3	30.13	4	200-275	0.37	0.66	10.2	67.9	1.6		
		4e1	1.85	33.61	7	150-300	0.73	0.83	18.9	69.0	2.2		
		4f1	2.35	26.64	6	150-275	0.6	0.79	11.5	67.4	2.8		
		4g1	2.85	33.43	6	150-275	0.65	0.79	23.2	68.6	1.5		
		4h1	3.35	38.03	5	150-250	0.53	0.75	5.2	64.9	5.1		
		4i1	3.85	38.44	5	150-250	0.52	0.75	5.7	66.1	4.5		
		4j1	4.45	39.43	5	150-250	0.48	0.75	5.2	77.9	5.4		
		2a1	0.45	5.71	5	200-375	0.47	0.69	4.9	72.4	4.8		
		2b1	0.55	22.17	6	175-300	0.51	0.79	7.3	71.5	3.0		
		2c1	1.15	29.32	5	150-300	0.62	0.82	14.9	77.5	2.6		
		2f1	2.7	34.72	5	150-250	0.54	0.74	5.1	63.3	5.0		
		2g1	3.25	36.24	5	150-250	0.53	0.74	8.6	65.2	3.0		
		2h1	4.0	35.34	3	200-250	0.28	0.50	2.3	62.2	3.5		
		2i1	4.35	37.50	5	150-250	0.51	0.75	10.9	65.7	2.0		
3349-2	5/5	492-1	0	0.155	5	150-340	0.485	0.741	18.3	33.4	0.7		
		492-2	0	0.020	5	150-340	0.523	0.738	9.5	34.2	1.4		
		492-3b	0	0.057	3	150-240	0.294	0.461	87.7	35.9	0.1		
		492-3	0	0.021	6	150-340	0.486	0.747	11.7	32.5	1.0		
		492-4	0	0.021	6	150-340	0.545	0.76	7.4	36.4	2.0	34.5	0.7
3349-2B	4/5	3349-2B	0.25	0.196	10	100-280	0.611	0.837	23.8	31.0	0.6		
		3349-2C	0.8	1.563	6	100-200	0.609	0.759	20.2	35.0	0.8		
		3349-2D	1.3	3.007	8	100-240	0.621	0.835	24.7	37.9	0.9		
		3349-2E	2.05	4.692	7	100-220	0.495	0.831	11.2	38.0	1.4		
3346-15	3/3	4615-1	0	0.014	6	25-340	0.866	0.789	68.8	38.0	0.4		
		4615-2	0	0.019	5	150-340	0.603	0.748	12.7	37.7	1.4		
		4615-3	0	0.005	5	25-290	0.698	0.728	71.5	34.1	0.2	36.6	1.2
3346-15A1	8/8	3346-15A1	0.25	0.234	6	25-250	0.855	0.772	77.4	33.3	0.3		
		3346-15A2	0.5	0.088	11	100-320	0.764	0.895	42.6	36.3	0.6		
		3346-15B	1	0.802	10	100-280	0.717	0.855	25.0	39.6	1.0		
		3346-15C	1.5	4.452	7	100-220	0.57	0.831	12.0	42.0	1.7		
		3346-15D	2	5.675	7	100-220	0.563	0.829	9.6	39.6	1.9		
		3346-15E	2.75	7.252	7	100-220	0.612	0.825	8.2	37.8	2.3		
		3346-15F	3.75	6.265	8	100-240	0.676	0.854	12.5	32.0	1.5		
		3346-15G	4.75	9.025	7	120-240	0.585	0.827	12.1	33.5	1.3		
3344-6	3/3	<i>Mean</i>										36.5	0.8
	11/11	3344-6a	0.25	0.156	11	120-340	0.689	0.879	42.2	33.0	0.5		
		3344-6b	0.75	3.650	8	25-240	0.689	0.832	16.1	44.6	1.6		

Table 1. (continued)

Sample	Success Rate ^a	Subsample ^b	Distance From Glassy Margin, cm	NRM, 10 ⁻³ A. m ² /kg	Number of Heating Steps Used	Temperature Range, deg. C	Fraction Factor	Gap Factor	Quality Factor	F _{as} , μT	Standard Error, μT ^d	F _{tot} ^e , μT	Standard Error, μT ^f
		3344-6c	1.25	7.892	6	120-215	0.386	0.794	6.2	48.7	2.4		
		3344-6d	1.75	8.650	6	120-215	0.459	0.792	5	47.1	3.4		
		3344-6e	2.5	8.361	6	120-215	0.503	0.792	7.6	47.4	2.5		
		3344-6f	3.5	7.428	6	120-215	0.506	0.791	4.5	44.5	4.0		
		3344-6g	4.5	5.916	6	120-215	0.561	0.787	21.6	35.8	0.7		
		3344-6h	5.5	5.464	6	120-215	0.571	0.783	10.0	33.0	1.5		
		3344-6i	6.5	6.381	6	120-215	0.583	0.743	14.5	33.8	1.0		
		3344-6j	7.5	5.507	6	120-215	0.579	0.786	12.5	29.5	1.1		
		3344-6k	8.5	9.585	6	120-215	0.596	0.786	20.3	37.9	0.9		

^aRate is for the glasses and the crystalline subsamples.
^bItalic values are for the glasses; bold values are for the glasses already measured by *Carlut and Kent* [2000]. “Mean” denotes a mean value obtained on several subsamples with individual values measured by *Carlut and Kent* [2000].

^cF_a denotes paleointensity.
^dValues are for individual specimens.
^eF_{tot} is unweighted mean paleointensity.
^fValues are for individual site/flow.

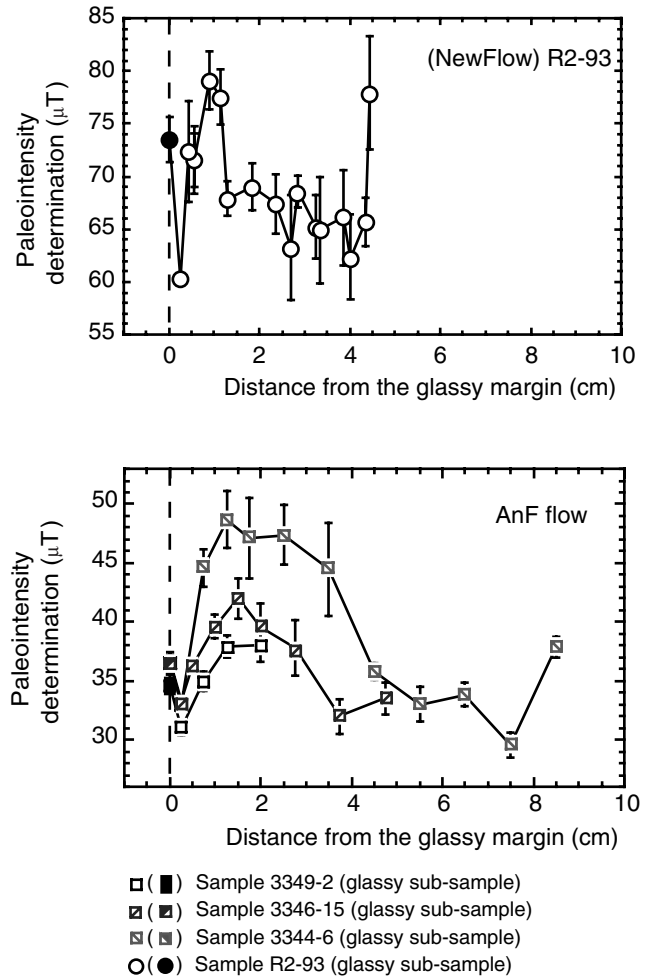


Figure 3. Individual paleointensity results obtained from R2-93 and Animal Farm subsamples plotted versus subsamples distance from the glassy margin. Error bars are associated standard errors.

(measured using a Bartington susceptibility meter) follows roughly the same trend as the NRM, the MORB fragments ranging from under the detection threshold in the glasses to 1×10^{-5} m³/kg in the inner part.

4.2. Curie and Unblocking Temperature and Magnetic Population

[11] Curie temperatures were performed on sample R2-93 using a horizontal Curie balance. Samples were heated in a 0.15 T field until 700°C at 50°/min in air. Curie temperatures were determined using the tangent method [*Grommé et al., 1979*] and range from 118° to 449°C for the heating curve (see Figure 5a). The behavior of all samples heated to 700° is highly nonreversible, reflecting the destruction and creation of magnetic mineral at high temperature (presumably due to the oxi-exsolution of titanomagnetite). The important issue is to know at which temperature the irreversible transformation occurs. If this temperature is less than the maximum temperature used for paleointensity determination, then this will preclude the recovery of accurate values. Twin samples were used to duplicate the thermomagnetic experiments but to temperatures only slightly above the maximum temperature (usually 300°C) used for the paleointensity determinations. Results show that curves are now reversible (for some samples a slight increase of the acquisition is noticeable), which is consistent with the observa-

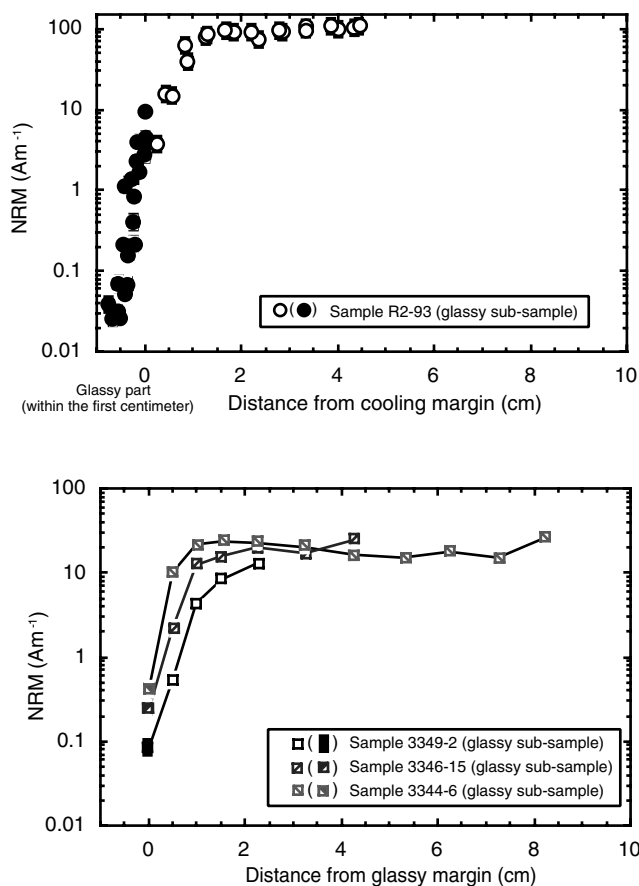


Figure 4. Individual NRMs from a collection of R2-93 and Animal Farm subsamples plotted versus subsample distance from the glassy margin.

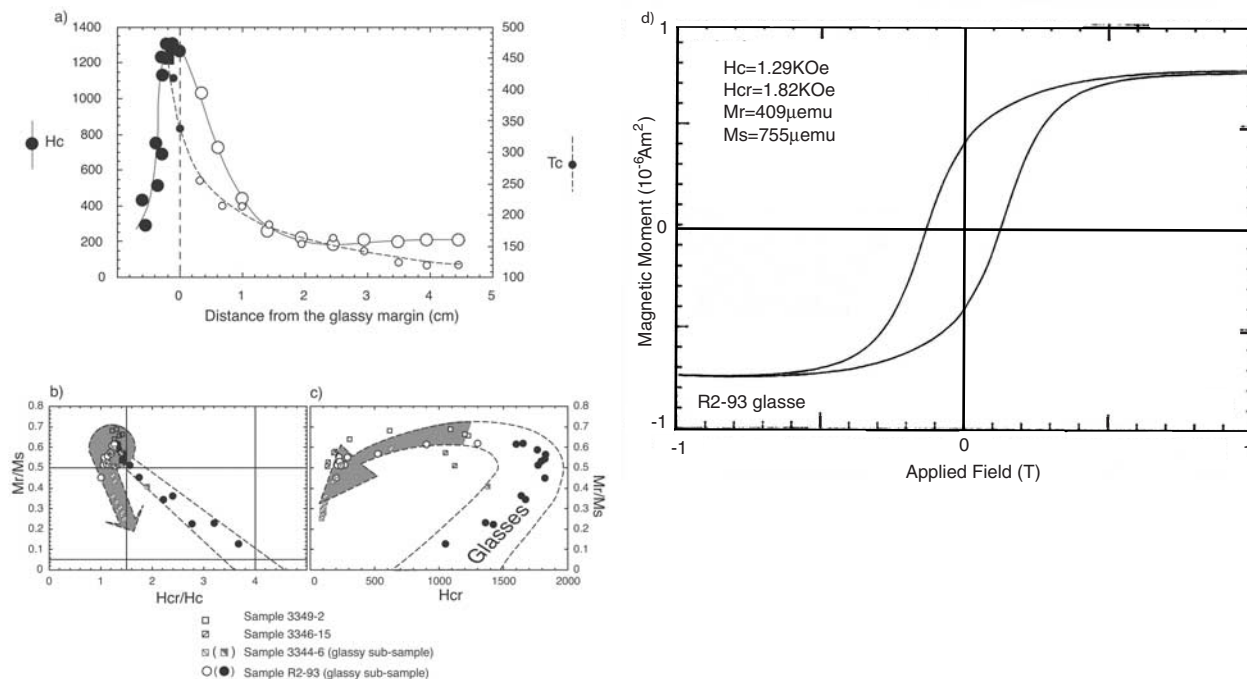


Figure 5. (a) Variations of hysteresis parameters H_c and Curie temperature T_c in sample R2-93 with depth. (b) Day diagram showing H_{cr}/H_c versus M_r/M_s for Animal Farm and R2-93 subsamples. The shaded areas correspond to a gross separation between superparamagnetism-single domain and multidomain behavior (see Figure 7). (c) H_{cr} versus M_r/M_s representation for the same batch of subsamples (d) Typical hysteresis loop using a Micromag 2900 for a glassy sample. A standard correction was applied for high field paramagnetic slope from 0.7 to 1.0 T.

tions of positive PTRM checks in the paleointensity experiments. Similar observations were made by *Pick and Tauxe* [1993] on Cretaceous submarine glasses where alterations in thermomagnetic experiments were found to occur only after the NRM unblocking temperature. Unblocking temperatures range from almost 580°C for the outer glasses to 380°C for the innermost samples. A significant fraction of NRM unblocking occurs above the Curie point, a phenomenon previously observed in young oceanic basalts by *Kent and Gee* [1994, 1996], who interpreted it as reflecting low-temperature oxidation. However, it now seems likely that this difference in temperature is probably due to an effective variation of titanium content in the original titanomagnetite [Zhou *et al.*, 1997, 2000]. Our results are consistent with a population of titanomagnetites grain with low titanium content close to the rim reaching progressively a value of titanomagnetite (TM) 60 (i.e., a uniform $Fe_{2.4}Ti_{0.6}O_4$ assemblage) in the interior.

[12] A more detailed description of the magnetic population in a sample from the 1993 flow has been reported by *Zhou et al.* [2000] using transmitted electronic microscopic observations. Jointly with chemical analyses [Zhou *et al.*, 1997], the observations converge toward the identification of two distinct magnetic grain populations. A groundmass population (hereinafter referred to as population A) of titanomagnetite grains with a composition converging to TM 60 and with sizes in the range 1–40 μm depending on the depth of observation with only the smaller grains observed near the cooling margin. A second population (population B) of very fine single domain-superparamagnetic (SD-SP) titanomagnetite grains has been reported [see also *Smith*, 1979] within amorphous interstitial glass and globules trapped within the matrix. These small particles are described as equidimensional and lie mostly in the range 0.03–0.1 μm (thus nearly pure SD). Their composition is not well constrained, with very low ulvospinel contents near the chilled rims of the samples and spanning a large range of ulvospinel contents in the interiors. No signs of alteration were found by

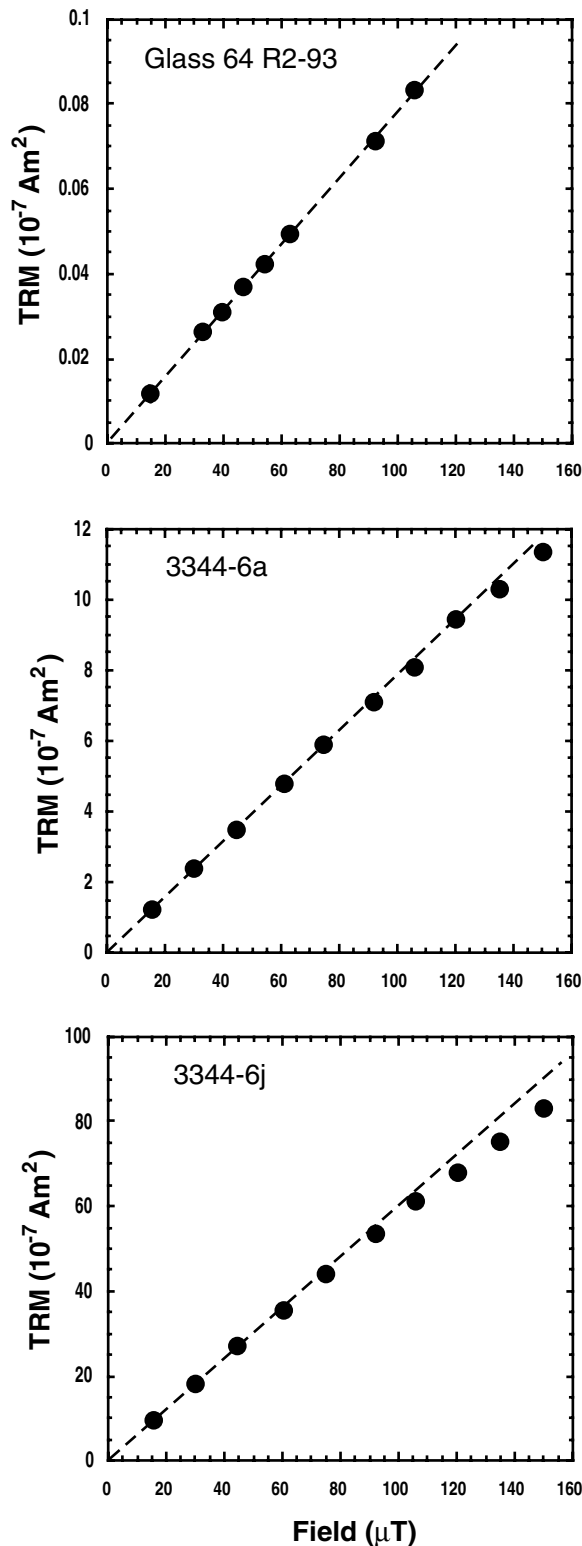


Figure 6. Evolution of acquired TRM in different laboratory fields varying from 15 to 145 μT .

Zhou *et al.* [2000] on this very young material even at a few millimeters from the margin.

4.3. Hysteresis Parameters

[13] Hysteresis measurements were made with an alternating gradient force magnetometer (Micromag 2900) on 13 glasses

(12 from R2-93 and 1 from 3344-6) and 30 nonglassy samples from the AnF and R2-93 flows. Glasses were difficult to measure because of their low magnetization. The obvious cooling rate dependence in the MORB fragments would predict a grain size sequence going from ultrafine, near superparamagnetic grains at the glassy margin, to a coarse, near multidomain population in the interior. Results are reported in Figure 5b on a Day (H_{cr}/H_c versus M_r/M_s) diagram. The outermost glasses give a range of hysteresis parameters that might be interpreted as characteristic of either pseudo-single or multidomain (MD) grains (i.e., a high H_{cr}/H_r ratio jointly with a low M_r/M_s value) on a Day diagram. However, in this case it is more likely the signature of very fine (rapidly cooled) superparamagnetic grains as already discussed by Gee and Kent [1996] and Zhou *et al.* [2000]. Some of the innermost basalts have a large M_r/M_s values above 0.5, which might be considered representative of a pure single-domain magnetic population. However, a high M_r/M_s value in MORB does not preclude a significant proportion of MD grains in the matrix. This is because of a dominant cubic anisotropy which would require a reevaluation of the SD threshold value of M_r/M_s , in this case above 0.8 [Joffe and Heuberger, 1974; Gee and Kent, 1995]. These ambiguities show that the use of Day diagrams to infer the size of the magnetic population in MORB samples is delicate. In particular, most interior subsamples lie at the top left corner of the diagram corresponding to very high M_r/M_s and low H_{cr}/H_r , despite a significant range in grain size revealed by microscopic observations [Zhou *et al.*, 2000]. The samples are more clearly distinguishable with a representation showing H_{cr} versus M_r/M_s as plotted in Figure 5c. Hysteresis parameters added to microscopic observations suggest that SP-SD grains (corresponding to high H_{cr} and low to very high M_r/M_s) are present within the glasses, whereas contributions from MD grains (low H_{cr} and moderate to low M_r/M_s) become evident within the rest of the basalt samples. We do not see any systematic constriction or wasp-waisted shape [Tauxe *et al.*, 1996] in the hysteresis curves in either the glass (or basalt) samples (e.g., Figure 5d); but in any case, constriction of hysteresis loops may not be a good indicator of any particular magnetic grain size distribution [Gee and Kent, 1999].

5. Testing the Magnetic Properties of the Samples

[14] In the following we investigate some of the underlying principles of the Thellier method: (1) the linearity between magnetization and field, (2) the reciprocity law between unblocking and blocking temperature, and (3) the influence of cooling rates.

5.1. Linearity Between Field and Magnetization

[15] Weak field TRM of lavas is expected to be linearly related to the applied field. As the laboratory field value is usually not the same as the paleofield, any disparity from linearity would cause a bias in the paleointensity result. The linearity has already been tested on various material [e.g., Dunlop and Özdemir, 1997] but not specifically on submarine basalts to our knowledge.

[16] A batch of samples from R2-93 and 3344-6 were heated at 250°C for the glassy subsamples and 185°C for the crystalline subsamples for 2 hours and cooled in zero field. The samples were then heated several successive times at 250° and 185°C, respectively, for 40 min and successively cooled in different fields between 15 and 145 μT . Typical results are shown in Figure 6. Glassy or near glassy samples (such as Glass 64 and 3344-6a in the top and middle plots, respectively of Figure 6) show good linearity between field and TRM over the whole field range. In contrast, samples from the pillow interior (e.g., 3344-6j at ~ 7.5 cm from the margin shown in the bottom of Figure 6) show an obvious nonlinearity in acquisition (above about 95 μT).

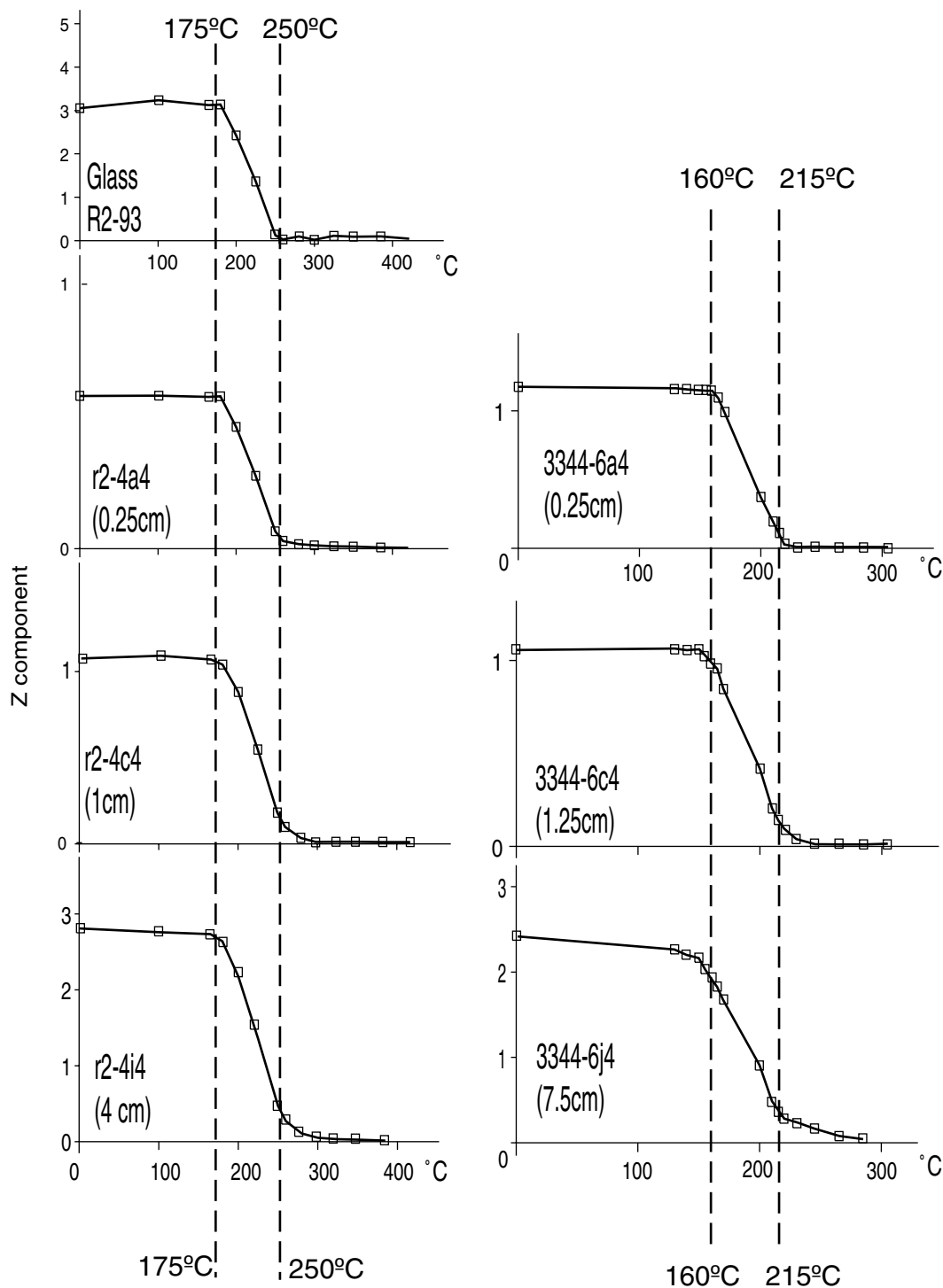


Figure 7. Demagnetization of the Z component induced in temperature intervals 175°–250°C and 160°–215°C shown for seven subsamples from R2-93 and 3344-6.

However, the effect is relatively small, only about 10% or less, and takes place well above the environmental present-day value of the field and thus should not be considered as a major factor preventing proper paleointensity values to be obtained from MORBs.

5.2. Reciprocity Law

[17] Another critical requirement for Thellier experiments is that the partial TRM acquired between any temperature interval [T-low; T-high] is thermally demagnetized over the exact same

interval when heated in zero field. Such a behavior was predicted by Néel theory and demonstrated by *Thellier* [1938] on single-domain grain assemblages but does not apply to multidomain grains [e.g., *Shcherbakov et al.*, 1993; *Xu and Dunlop*, 1994; *Dunlop and Özdemir*, 1997].

[18] Two experiments were performed with R2-93 and 3344-6 samples. Samples were slowly cooled from an upper temperature (T-high in the following) equal to 250°C (for R2-93) or 215°C (for 3344-6 samples) to a lower temperature (T-low in the following) equal to 175°C (R2-93) or 160°C (3344-6) in a

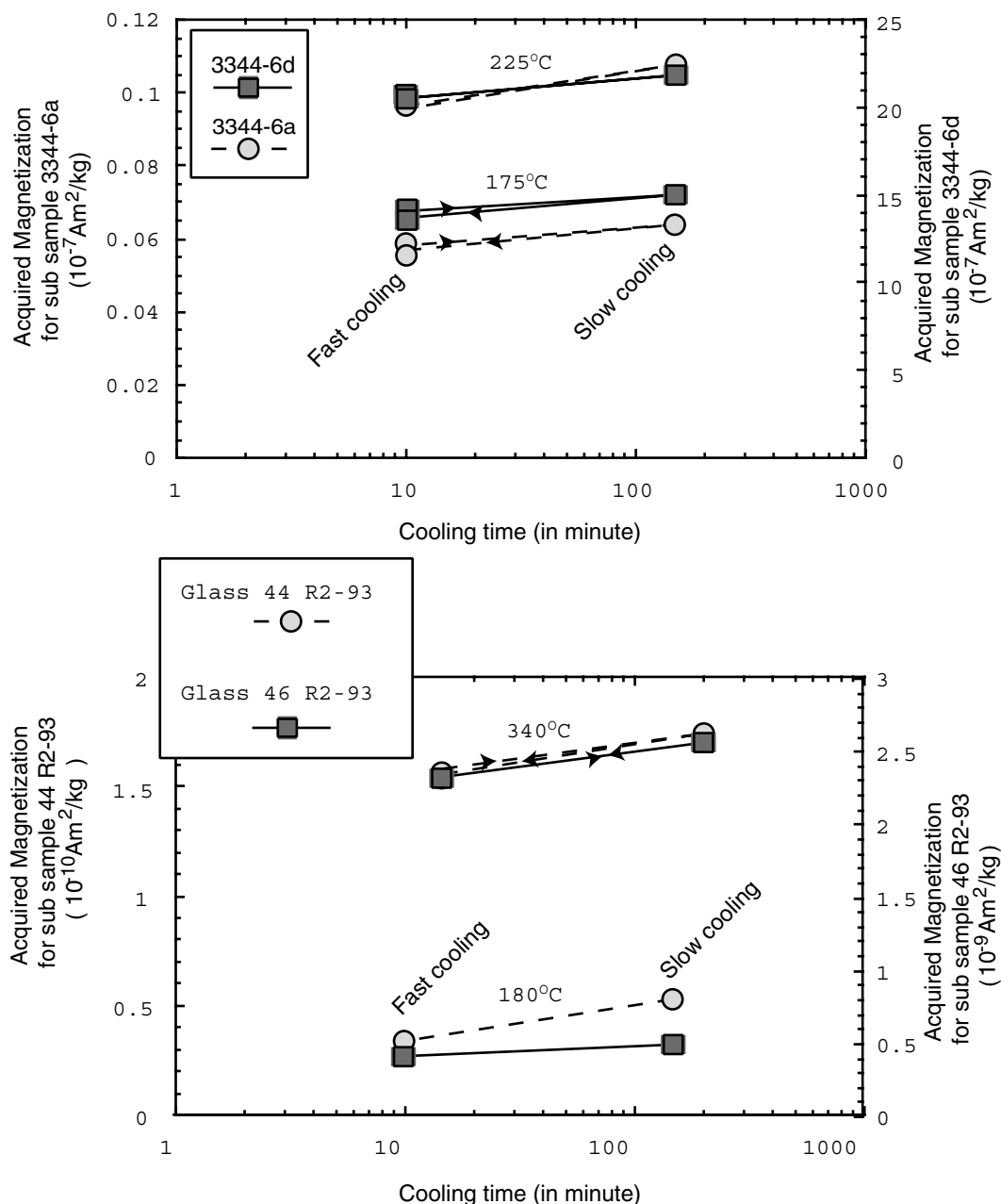


Figure 8. Acquisition of magnetization as a function of cooling rate for four subsamples in a field of $40 \mu\text{T}$.

laboratory field of $40 \mu\text{T}$ along a z axis chosen to be perpendicular to samples NRM (oriented in the x - y plane). Below T-low the cooling was in zero field until room temperature. The samples were then progressively thermally demagnetized, the demagnetization of 3344-6 being especially detailed (at 5°C interval close to T-low and T-high).

[19] Representative results of the value of the Z component are shown in Figure 7. In the glass (one sample from R2-93) and first nonglassy sample (r2-4a4 and 3344-6A4), the Z component is, as expected, demagnetized between 175°C and 250°C , with sharp changes in the slope marking the temperatures at which the field was imposed and suppressed. The next samples are associated with a smoother curve, demagnetization starting before reaching T-low ($\sim 10^\circ\text{C}$ before) and ending slowly after T-high ($\sim 20^\circ\text{C}$ higher) (as r2-4c4 and 3344-6c4 in Figure 7). Getting deeper into the samples, a clear degradation occurs as illustrated by the results shown in subsamples r2-4i4 and 3344-6j4, where the demagnetization starts some 30°C prior to T-low and ends

40°C to almost 80°C above T-high. This experiment clearly shows that a continuous spectrum of unblocking temperature is associated with a single sharp blocking temperature in crystalline subsamples from more than 1 cm distance from the cooling margin. This behavior, leading to overlapping and therefore nonreciprocity of partial TRM, will preclude the recovery of accurate paleointensity values using the Thellier method on such material.

5.3. Influence of the Cooling Rate

[20] Theoretical as well as experimental studies by several authors [Dodson and McClelland Brown, 1980; Halgedahl et al., 1980; Fox and Aitken, 1980; McClelland Brown, 1984; Chauvin et al., 1991] have shown that the magnitude of a TRM acquired by magnetite or titanomagnetite grains, particularly single-domain populations, is affected by the rate at which the sample is cooled. In the case of Thellier experiments this can be very critical if the rate of the laboratory cooling is different than in

nature, which is usually the case. Following kinetic theories of magnetization, a stronger TRM is expected to be associated with slowly cooled samples [e.g., *Dodson and McClelland Brown*, 1980; *Halgedahl et al.*, 1980]. However, the opposite effect (i.e., a slow cooled TRM weaker than a fast cooled TRM) was subsequently reported by *McClelland Brown* [1984] on SD magnetite and MD titanomagnetite (TM 30) samples and was interpreted as being due to interaction effects between particles in magnetite-rich inclusions.

[21] A batch of glassy and nonglassy samples were cooled at different rates in a lab field of 40 μ T. Coolings were performed from 180°C and 340°C to room temperature for the glassy samples and from 175°C and 225°C to room temperature for the nonglassy samples. After the first heating, samples were cooled as rapidly as possible at a rate of $\sim 25^\circ\text{C}/\text{min}$ using forced air. The experiment was then repeated with a slow cooling rate of $\sim 2^\circ\text{C}/\text{min}$ using conductive cooling in the sealed oven. In order to check for any possible magneto-chemical alteration during heating which could interfere with the experiment, a final fast cooling was performed, and the result was compared with the first one. It appears that all samples are sensitive to cooling rate (Figure 8) with a slow cooling rate associated with stronger acquisition, as expected from theoretical considerations. The difference can be on the order of 15% for the glasses and 10% for the nonglassy samples. This result highlights another significant drawback of the Thellier method on MORBs and implies that it might only be possible to recover a proper value of intensity when the laboratory cooling is very similar to in situ cooling.

6. Discussion

[22] Anomalous high paleointensity values were found within a few centimeters of the chilled margin in seemingly ideal, fresh, rapidly cooled MORB material. This result can hardly be explained by in situ alteration as observations using scanning electron microscopy (SEM) show that no alteration is present on this very recent material [*Zhou et al.*, 2000]. Laboratory alteration is also difficult to advocate because the experimental behavior is very good with positive checks.

[23] In all samples, important variations in magnetic properties on very small scales were found. Overlaps of TRM spectrums were revealed by our experiments on samples from pillow R2-93 and lobate 3344-6 as close as 1 cm from the glassy margin of the samples. Nonreciprocity of partial TRM is usually associated with the presence of MD grains [*Dunlop and Özdemir*, 1997]. Typical MD behavior was not expected a few centimeters from the cooling margin in this material but is consistent with SEM observations made on a sample from the New Flow. A sharp increase in grain size population occurs within the first centimeters of the pillow rim, leading to the presence of grains in the 4 μ m range at only 1 cm from the glassy margin [*Zhou et al.*, 2000]. Furthermore, no signs of internal subdivision by intergrowth of smaller grains within the coarser grains are observed (see transmission electron microscopy experiments by *Evans and Wayman* [1972] and *Smith* [1979]). Hence an effect of the rapid cooling is the absence of initial high-temperature oxidation which occurs widely in much more slowly cooled subaerial basalts, leading to the emergence of a demixed population of high-Ti and low-Ti elongated, small, uniaxial, grains. This process has been advocated to be responsible for most of the paleomagnetic behavior in subaerial lavas [*Strangway et al.*, 1968; *Dunlop and Özdemir*, 1997]. The cubic anisotropy revealed in our experiments by the high M_r/M_s ratio of 0.7 or more [see also *Gee and Kent*, 1995] also attests to the absence of high-temperature oxidation. Titanomagnetite grains within the crystalline interior have not experienced subdivision, and their homogeneity

can account for the high M_r/M_s ratio and MD behavior as little as 1 cm after the glassy margin.

[24] Results from the cooling rate experiments indicate that a difference of only 1 order of magnitude in the cooling rate of the subsamples leads to significant difference in the magnitude of acquired magnetization. The presence of glasses implies a cooling dominated by convection of seawater at a rapid rate of more than $10^\circ\text{--}60^\circ\text{C}/\text{s}$ [*Heiken et al.*, 1991]. The cooling of the glassy crust from the Curie temperature to 100°C should thus take place in less than a few seconds. Within the crystalline flow interiors the cooling is dominated by thermal diffusion and is associated with a much slower rate. Precise cooling rate estimates will depend on the size of the flow and the possible circulation of seawater in cavities within the flow. Nevertheless, in our case an estimate of a few minutes for the first centimeter of the crystalline part and a few tens of minutes to a few hours deeper into the flow [after *Fink and Griffiths*, 1990] is reasonable. This result indicates that sample a (shown in Figure 1, closest to the rim) could be the only sample to have the same cooling rate during the laboratory experiment and in nature. As sample a in our experiments does not show signs of MD behavior, it is possibly the best “compromise” candidate to recover paleointensity using the Thellier method.

6.1. Pattern Observed After Sample a

[25] A strong increase in paleointensity results is observed on a millimeter scale after sample a. The cooling rate difference between experiments in the laboratory and in situ cooling is not expected to be critical close to the rim of the flow and thus could hardly be responsible for significant paleointensity increase on such a small scale. More likely, interactions between magnetic domains appear quickly as the proportion of MD grains increases on a millimeter scale inside the crystalline part and yields inconsistent values. The steep increase of the paleointensity results implies a sharp threshold between SD and MD behavior.

[26] After a few centimeters a decrease in paleointensity occurs, leading to average values close to sample a and glassy samples values. The structure of the pattern (intensity increasing and decreasing) indicates that competitive effects are present, probably involving cooling rate difference and increase in magnetic interactions due to a larger proportion of MD grains.

6.2. Decrease Between Glasses and Sample a

[27] In all cases reported here, there is a tendency for a decrease in paleointensity values between the glasses and sample a. It is difficult to know from this limited set of data if this is a representative phenomenon and which of the two values (glasses or sample a) is the closest to the intensity of the ambient magnetic field during the time of the cooling. Even in the case of the precisely dated 1993 New Flow local, local magnetic anomalies are present, and the resultant ambient intensity may depart from the geomagnetic reference value by some microtesla [*Carlut and Kent*, 2000]. Furthermore, the anomalously high FeO* content of the New Flow makes it very atypical in terms of magnetic properties [see, e.g., *Tivey et al.*, 1998]. For the AnF flow, *Carlut and Kent* [2000] have used the paleointensity value of $35.6 \pm 1 \mu\text{T}$ obtained from the glasses of AnF to infer an age for this flow by comparison with calibrated reference curves (definitive geomagnetic reference field). Following this method, the AnF flow was given an age between 1890 and 1940 A.D. in broad accordance with in situ observations. However, when averaged, the three “a” samples give a value of $32.4 \pm 1.4 \mu\text{T}$ that is not discernable, given the error bars, from the value of today’s field at this location (31.2 μT according to the international geomagnetic reference field 2000), leading to an age younger than 1950 A.D. for this flow. This result is also in accordance with in situ observations.

[28] New results obtained recently on ten other East Pacific Rise pillow and lobate flows [Carlut *et al.*, 2001; Cormier *et al.*, 2001] show that there is probably no systematic differences in the paleointensity values obtained on glasses and on the more slowly cooled first few millimeters of the cryptocrystalline part (called sample a in this paper). This strengthens the confidence in paleointensity results obtained on the outermost part of the flows, whether it is glassy or not, as long as it contains mainly SP to SD populations. Nevertheless, nonglassy samples should be used very carefully because of the extremely rapid transition between SD and MD behavior found in submarine samples.

7. Conclusion

[29] Our study demonstrates that recent MORBs, in general, might be unsuitable for paleointensity determination, giving values up to 50% higher than expected. Despite high M_r/M_s values, usually associated with pure SD populations, typical MD behavior was observed at a few millimeters from the cooling margin inside the pillow and lobate samples analyzed. This result is in accordance with SEM observations made by Zhou *et al.* [2000] showing the presence of titanomagnetite grains a few micrometers in size as close as 1 cm from the chilled glassy rim. The absence of high-temperature oxidation in submarine basalts might be responsible for the occurrence of a MD grains population with cubic anisotropy, as revealed by the high M_r/M_s values but which nevertheless failed in passing the reciprocity law test. Such a population could dominate the magnetic behavior of submarine basalts which would therefore behave in a very different manner than subaerial basalts where exsolution almost always occurs. The most discordant paleointensity values are found where the grain size population is near the threshold between SD and MD, accounting for high magnetizations but wrong values. This surprising result attests to the extremely rapid transition between SD and MD behavior. While the inner part of submarine basalts is extremely difficult to use because of MD effects, the glassy part of the sample and the first cryptocrystalline sample close to the chilled margin could lead to a correct evaluation of the field intensity and are associated with a single population of fine single-domain grains. Marine magnetic anomalies could still provide a reliable record of the past intensity variations of the field as natural remanent magnetization may still be representative of intensity, as shown by Gee *et al.* [2000] and Pouliquen *et al.* [2001].

[30] **Acknowledgments.** We are grateful to David Dunlop and Lisa Tauxe for their helpful reviews of the paper. We thank Milene Cormier, Jeff Gee, John Sinton, and H. Paul Johnson for discussions, help, and providing us with samples. Research supported by the U.S. National Science Foundation grant OCE-0002563 and a Lamont-Doherty Post-doctoral Fellowship (JC). LDEO contribution 6258.

References

Auzende, J.-M., J. Sinton, and S. Party, NAUDUR explorers discover recent volcanic activity along the East Pacific Rise, *EOS Trans. AGU*, 75(601), 604–605, 1994.
 Auzende, J.-M., *et al.*, Recent tectonic, magmatic, and hydrothermal activity on the East Pacific Rise between 17°S and 19°S: Submersible observations, *J. Geophys. Res.*, 101, 17,995–18,010, 1996.
 Cande, S. C., and D. V. Kent, Ultrahigh resolution marine magnetic anomaly profiles: A record of continuous paleointensity variations?, *J. Geophys. Res.*, 97, 15,075–15,083, 1992.
 Carlut, J., and D. V. Kent, Paleointensity record in zero-age submarine basalt glass: Testing a new dating technique for recent MORBS, *Earth Planet. Sci. Lett.*, 389–401, 2000.
 Carlut, J., D. V. Kent, and M. H. Cormier, Paleointensity Experiments on MORBs from the northern East Pacific Rise, *EOS Trans. AGU*, 82(47), Fall Meet. Suppl., Abstract no. GP41A-0252, 2001.
 Chauvin, A., P.-Y. Gillot, and N. Bonhommet, Paleointensity of the Earth's magnetic field recorded by two late quaternary volcanic sequences at the island of La Réunion (Indian Ocean), *J. Geophys. Res.*, 96, 1981–2006, 1991.

Chauvin, A., Y. Garcia, P. Lanos, and F. Laubheimer, Paleointensity of the geomagnetic field recovered on archaeomagnetic sites from France, *Phys. Earth Planet. Int.*, 120, 111–136, 2000.
 Coe, R. S., Paleointensities of the Earth's magnetic field determined from Tertiary and Quaternary rocks, *J. Geophys. Res.*, 72, 3247–3262, 1967.
 Coe, R. S., S. Gromme, and E. A. Mankinen, Geomagnetic paleointensities from radiocarbon-dated lava flows on Hawaii and the question of the Pacific nondipole low, *J. Geophys. Res.*, 83, 1740–1756, 1978.
 Cormier, M. H., J. Carlut and D. V. Kent, Preliminary paleointensity results obtained along two adjacent ridge segments of the east Pacific Rise (15°N–17°N), *EOS Trans. AGU*, 82(47) Fall Meet. Suppl., Abstract no. T12A-0905, 2001.
 Dodson, M. H., and E. McClelland Brown, Magnetic blocking temperatures of single-domain grains during slow cooling, *J. Geophys. Res.*, 85, 2625–2637, 1980.
 Dunlop, D. J., and C. J. Hale, A determination of paleomagnetic field intensity using submarine basalts drilled near the Mid-Atlantic Ridge, *J. Geophys. Res.*, 81, 4166–4172, 1976.
 Dunlop, D., and O. Özdemir, *Rock Magnetism*, 573 pp., Cambridge Univ. Press, New York, 1997.
 Evans, M. E., and M. L. Wayman, The Mid-Atlantic ridge near 45°N, XIX, An electron microscope investigation of the magnetic minerals in basalt samples, *Can. J. Earth Sci.*, 9, 671–678, 1972.
 Fink, J. H., and R. W. Griffiths, Radial spreading of viscous-gravity currents with solidifying crust, *J. Fluid Mech.*, 221, 485–500, 1990.
 Fox, C. G., W. E. Radford, R. P. Dziak, T.-K. Lau, H. Matsumoto, and A. E. Schreiner, Acoustic detection of a seafloor spreading episode on Juan de Fuca ridge using military hydrophone arrays, *Geophys. Res. Lett.*, 22, 131–134, 1995.
 Fox, J. M. W., and M. J. Aitken, Cooling rate dependence of thermoremanent magnetization, *Nature*, 283, 462–463, 1980.
 Gee, J., and D. V. Kent, Magnetic hysteresis in young mid-ocean ridge basalts: Dominant cubic anisotropy?, *Geophys. Res. Lett.*, 22, 551–554, 1995.
 Gee, J., and D. V. Kent, Calibration of magnetic granulometric trends in oceanic basalts, *Earth Planet. Sci. Lett.*, 170, 377–390, 1999.
 Gee, J., D. A. Schneider, and D. V. Kent, Marine magnetic anomalies as recorders of geomagnetic intensity variations, *Earth Planet. Sci. Lett.*, 144, 327–335, 1996.
 Gee, J. S., S. C. Cande, J. A. Hildebrand, K. Donnelly, and R. L. Parker, Geomagnetic intensity variations over the past 780 kyr obtained from near-seafloor magnetic anomalies, *Nature*, 408, 827–832, 2000.
 Griffiths, R. W., and J. H. Fink, Solidification and morphology of submarine lavas: A dependence on extrusion rate, *J. Geophys. Res.*, 97, 19,729–19,737, 1992.
 Grommé, S., E. A. Mankinen, M. Marshall, and R. S. Coe, Geomagnetic paleointensities by the Thelliers' method from submarine pillow basalts: Effects of seafloor weathering, *J. Geophys. Res.*, 84, 3553–3575, 1979.
 Halgedahl, S. L., R. Day, and M. Fuller, The effect of cooling rate on the intensity of weak-field TRM in single-domain magnetite, *J. Geophys. Res.*, 85, 3690–3698, 1980.
 Heiken, G. H., D. T. Vaniman, and B. M. French, *Lunar Sourcebook: A Users Guide to the Moon*, 736 pp., Cambridge Univ. Press, New York, 1991.
 Joffe, I., and R. Heuberger, Hysteresis properties of distributions of cubic single-domain ferromagnetic particles, *Philos. Mag.*, 29, 1051–1059, 1974.
 Johnson, H. P., and M. A. Tivey, Magnetic properties of zero-age oceanic crust: A new submarine lava flow on the Juan de Fuca ridge, *Geophys. Res. Lett.*, 22, 175–178, 1995.
 Kent, D. V., and J. Gee, Grain size-dependent alteration and the magnetization of oceanic basalts, *Science*, 265, 1561–1563, 1994.
 Kent, D. V., and J. Gee, Magnetic alteration of zero-age oceanic basalt, *Geology*, 24, 703–706, 1996.
 Marshall, M., and A. Cox, Magnetism of pillow basalts and their petrology, *Geol. Soc. Am. Bull.*, 82, 537–552, 1971.
 McClelland Brown, E., Experiments on TRM intensity dependence on cooling rate, *Geophys. Res. Lett.*, 11(3), 205–208, 1984.
 Mejia, V., N. D. Opdyke, and M. R. Perfit, Paleomagnetic field intensity recorded in submarine basaltic glass from the East Pacific Rise, the last 69 KA, *Geophys. Res. Lett.*, 23, 475–478, 1996.
 Nagata, T., Y. Arai, and K. Momose, Secular variation of the geomagnetic total force during the last 5000 years, *J. Geophys. Res.*, 68, 5277–5281, 1963.
 Pick, T., and L. Tauxe, Holocene paleointensities: Thellier experiments on submarine basaltic glass from the East Pacific Rise, *J. Geophys. Res.*, 98, 17,949–17,964, 1993.
 Pouliquen, G., Y. Gallet, P. Patriat, J. Dyment, and C. Tamura, A geomagnetic record over the last 3 million years from deep-tow magnetic anomaly profiles across the Central Indian Ridge, *J. Geophys. Res.*, 106, 10,941–10,960, 2001.
 Prévot, M., E. A. Mankinen, C. S. Grommé, and A. Lecaille, High paleoin-

- tensities of the geomagnetic field from thermomagnetic studies on rift valley pillow basalts from the Mid-Atlantic Ridge, *J. Geophys. Res.*, *88*, 2316–2326, 1983.
- Prévot, M., E. A. Mankinen, R. S. Coe, and C. S. Grommé, The Steens Mountain (Oregon) polarity transition, 2, Field intensity variations and discussion of reversal models, *J. Geophys. Res.*, *90*, 10,417–10,448, 1985.
- Shcherbakov, V. P., E. McClelland, and V. V. Shcherbakova, A model of multidomain thermoremanent magnetization incorporating temperature-variable domain structure, *J. Geophys. Res.*, *98*, 6201–6216, 1993.
- Smith, P. K. K., The identification of single-domain titanomagnetite particles by means of transmission electron microscopy, *Can. J. Earth Sci.*, *16*, 375–381, 1979.
- Strangway, D. W., E. E. Larson, and M. Goldstein, A possible cause of high magnetic stability in volcanic rocks, *J. Geophys. Res.*, *73*, 3787–3795, 1968.
- Tauxe, L., T. A. T. Mullender, and T. Pick, Potbellies, wasp-waists, and superparamagnetism in magnetic hysteresis, *J. Geophys. Res.*, *101*, 571–583, 1996.
- Theillier, E., Sur l'aimantation des terres cuites et ses applications géophysiques, *Ann. Inst. Phys. Globe Paris*, *16*, 157–302, 1938.
- Theillier, E., and O. Theillier, Sur l'intensité du champ magnétique terrestre dans le passé historique et géologique, *Ann. Geophys.*, *15*, 285–376, 1959.
- Tivey, M. A., H. P. Johnson, A. Bradley, and D. Yoerger, Thickness of a submarine lava flow determined from near-bottom magnetic field mapping by autonomous underwater vehicle, *Geophys. Res. Lett.*, *25*, 805–808, 1998.
- Valet, J. P., J. Brassart, I. LeMeur, V. Soler, X. Quidelleur, E. Tric, and P. Y. Gillot, Absolute paleointensity and magnetomineralogical changes, *J. Geophys. Res.*, *101*, 25,029–25,044, 1996.
- Xu, S., and D. J. Dunlop, Theory of partial thermoremanent magnetization in multidomain grains, 2, Effects of microcoercivity distribution and comparison with experiments, *J. Geophys. Res.*, *99*, 9025–9033, 1994.
- Zhou, W., R. Van der Voo, and D. R. Peacor, Single-domain and superparamagnetic titanomagnetite in young ocean-floor basalts with variable Ti-content, *Earth Planet. Sci. Lett.*, *150*, 353–362, 1997.
- Zhou, W., R. Van der Voo, and D. R. Peacor, Preservation of pristine titanomagnetite in older ocean-floor basalts and its significance for paleointensity studies, *Geology*, *27*, 1043–1046, 1999.
- Zhou, W., R. Van der Voo, D. Peacor, and Y. Zhang, Variable Ti-content and grain size of titanomagnetite as a function of cooling rate in very young MORB, *Earth Planet. Sci. Lett.*, *179*, 9–20, 2000.

J. Carlut, Laboratoire de Géologie ENS, 24, rue Lhomond 75231 Paris cedex 05, France. (jcarlut@ldeo.columbia.edu)

D. V. Kent, Paleomagnetism Laboratory, Lamont-Doherty Earth Observatory, Columbia University, 61 Route 9W, Palisades, NY 10964, USA. (dvk@ldeo.columbia.edu)